

Comparison and correlation of in vitro, in vivo and in silico evaluations of alpha, beta and gamma cyclodextrin complexes of curcumin

Nagaraju M. Patro · Azmi Sultana · Keiji Terao · Daisuke Nakata ·
Ayako Jo · Akihito Urano · Yoshiyuki Ishida · Raghu N. Gorantla ·
Vinay Pandit · Kshama Devi · Shishir Rohit · Baljinder K. Grewal ·
Elizabeth M. Sophia · Anand Suresh · Vineeth K. Ekbote · Sarasija Suresh

Received: 7 February 2013 / Accepted: 10 April 2013
© Springer Science+Business Media Dordrecht 2013

Abstract In the present study investigated the effect of curcumin (CUR) alpha (α), beta (β) and gamma (γ) cyclodextrin (CD) complexes on its solubility and bioavailability. CUR the active principle of turmeric is a natural antioxidant agent with potent anti-inflammatory activity along with chemotherapeutic and chemopreventive properties. Poor solubility and poor oral bioavailability are the main reasons which preclude CUR use in therapy. Extent of complexation was β -CD complex (82 %) > γ -CD (71 %) > α -CD (65 %). Pulverization method resulted in significant enhancement of CUR (0.002 mg/ml) solubility with CUR α -CD complex (0.364 mg/ml) > CUR β -CD complex (0.186 mg/ml) > CUR γ -CD complex (0.068 mg/ml). Gibbs-free energy and in silico molecular docking studies favour formation of α -CD complex > β -CD complex > γ -CD complex. With reference to CUR, relative bioavailability of CUR α -CD, CUR β -CD and CUR γ -CD complexes were 460, 365 and 99 % respectively. CUR-CD complexes exhibited increased bioavailability with an increase in $t_{1/2}$, t_{max} , C_{max} , AUC, K_a , and MRT; and a decrease in K_e , clearance and V_d values. AUC increase was CUR α -CD complex > CUR β -CD complex > CUR γ -CD complex. Significant difference ($p < 0.05$) was observed between CUR α -CD complex and CUR γ -CD complex by

one-way ANOVA and Dunnett's post hoc test for multiple comparison analysis. Correlation observed between in vitro, in vivo and in silico methods indicates potential of in silico and in vitro methods in CD selection.

Keywords Curcumin · Alpha cyclodextrin · Beta cyclodextrin · Gamma cyclodextrin · Solubility · Bioavailability

Introduction

Curcumin (CUR) or diferuloyl methane is a yellow polyphenol isolated from the rhizome of turmeric (*Curcuma longa*). From ancient times in Ayurveda (Indian system of medicine) turmeric has been used in treating sprains, inflammation, infections and hepatic disorders [1]. The active principle of turmeric, CUR, has shown therapeutic benefits in cardiovascular diseases [1], diabetes [2], Alzheimer's disease [3], multiple sclerosis [4], HIV [5], cataract [6] and inflammatory bowel disease [7]. Potent antioxidant and anti-inflammatory activity of CUR leads to an array of metabolic, cellular and molecular activities that individually or in combination exhibit diverse therapeutic activities including chemopreventive and chemotherapeutic activities [8–17]. CUR exhibits poor oral bioavailability and poor photostability which precludes its use in therapy despite its therapeutic potential. Poor water solubility and extensive pre-systemic and systemic metabolism of curcumin results are responsible for its poor oral bioavailability (1 % or lower) [18, 19].

Cyclodextrin (CD) inclusion complexation of drugs is an important method for increasing solubility of poorly water-soluble drugs [20]. CDs are cyclic (α -1,4)-linked oligosaccharides composed of α -D-glucopyranose residues.

N. M. Patro · A. Sultana · R. N. Gorantla · V. Pandit ·
K. Devi · A. Suresh · S. Suresh
Al-Ameen College of Pharmacy, Hosur Road,
Bangalore 560027, India

K. Terao · D. Nakata · A. Jo · A. Urano · Y. Ishida
Cyclochem Co., Ltd, Tokyo, Japan

S. Rohit · B. K. Grewal · E. M. Sophia ·
V. K. Ekbote · S. Suresh (✉)
National Institute of Pharmaceutical Education and Research
(NIPER), Mohali, Punjab, India
e-mail: ssuresh@niper.ac.in; sarasija_s@hotmail.com

Most common natural CDs are alpha CD (α -CD), beta CD (β -CD) and γ -CD consisting of six, seven and eight D-glucopyranose residues. CDs contain a relatively hydrophobic central cavity because of methane hydrogen atoms directed towards inside of the ring which is capable of entrapping hydrophobic molecules to form inclusion complexes; OH groups on the outside imparts hydrophilicity to CD molecule [21].

The research activity of CUR is intensively studied. A recent Medline search indicated over thousands of publications describing its various activities. However, studies on increasing oral bioavailability of CUR are not extensive. For instance, CUR-hydroxypropyl CD complex exhibited potent anti-inflammatory activity of CUR-hydroxypropyl CD complex in synthetic dextran sulphate induced rat colitis model [22]. We investigated the effect of CUR-CD complexes on CUR solubility and oral bioavailability. We hypothesized increasing solubility of CUR could decrease the extent of its pre-systemic and systemic metabolism and enhance bioavailability. We studied the effect of α -CD, β -CD and γ -CD complexes on CUR bioavailability. Pulverization technique, also called co-grinding, resulted in CD complexes with maximum CUR content and solubility with potential of scale-up for large scale manufacture. CUR-CD complexes were characterized by FTIR, X-ray diffractometry, DSC and ^1H -NMR studies. The in vitro dissolution behaviour of CUR and CD complexes was studied in simulated gastric fluid (SGF) and fasted state simulated intestinal fluid (FaSSIF) medium. The in vivo bioavailability of CUR and the CUR-CD complexes was evaluated in New Zealand rabbits. Further, computed IVIVC Level A correlation for CUR and CUR-CD complexes by linear regression analysis of a plot of percentage drug dissolved in vitro and percentage drug absorbed. Determined by in silico molecular modelling studies the most stable CUR-CD complex by determining the ease of docking CUR in CD molecule. A comparison of in silico data, Gibbs-free energy and in vivo results indicated the potential of in silico modelling studies in predicting the most favourable CD for formulation development.

Materials and methods

Curcumin (C3 complex) was a gift sample from Sami Labs Limited, Bangalore, India. Samples of α -CD (CAVAMAX W6), β -CD (CAVAMAX W7), γ -CD (CAVAMAX W8) were kindly provided by Cyclo Chem Ltd, Japan. Enzymes β -glucuronidase, type B-1 from bovine liver and sulfatase, type H-1 from *Helix pomatia* were procured from Sigma-Aldrich (Germany). Acetonitrile and methanol (HPLC grade) were procured from Merck, India. All the other solvents and reagents were of A.R. grade. All solutions were prepared using ultra pure water (MILLI Q, Millipore).

Estimation of CUR by HPLC

Developed a HPLC method of the estimation of CUR in Shimadzu HPLC system (Shimadzu, Japan) equipped with Shimadzu LC-10A pump and UV-Vis SPD-10 AVP detector. Selected Merck C18 (250×4.6 mm) column packed with 5 μm particles. Mobile phase consisted of a mixture of acetonitrile: tetrahydrofuran: 2 % acetic acid (50:30:20). Optimized flow rate at 1 ml/min to obtain 3.2 min retention time at ambient conditions at 423 nm. A linear calibration curve was obtained in 0.05–5 $\mu\text{g/ml}$ concentration range. Plotted the area under curve values versus concentration to obtain the following regression equation:

$$Y = 0.189X - 5.295 (R^2 = 0.999) \quad (1)$$

Phase-solubility studies

Conducted phase-solubility studies by Higuchi and Connors method to determine the stoichiometry of CUR-CD binary systems [23, 24]. Added an excess amount of CUR to different molar concentrations (2–8 mM) of α -CD, β -CD and γ -CD in 5 ml of distilled water (pH 5.5–6) to form saturated solutions at RT and agitated in Water Bath Shaker (Model RSB-12, REMI Laboratory Instruments, India) at 120–130 stokes/min for 2 h at 37 °C. Estimated CUR dissolved by HPLC at 423 nm after filtration of samples and suitable dilution with methanol (40 % v/v). Figure 1 presents the phase-solubility diagram obtained by plotting molar concentration of CD versus solubility of CUR. Calculated the apparent stability constant (K_s) from the slope of the phase-solubility diagram by Eq. 2.

$$K_s + \frac{\text{Slope}}{S_0(1 - \text{Slope})} \quad (2)$$

where S_0 is the solubility of curcumin in the absence of CD.

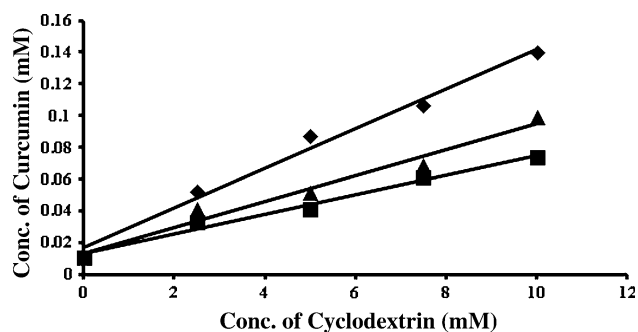


Fig. 1 Phase solubility profiles of curcumin in cyclodextrins in water. Mean \pm SD, $n = 3$; filled diamond alpha CD, filled square beta CD, filled triangle gamma CD

Calculated the Gibbs-free energies of transfer, ΔG_o , of CUR from an aqueous solution to cavity of CD using Eq. 3

$$G_0 = -2.303RT \log \left[\frac{S_0}{S_t} \right] \quad (3)$$

where S_0 and S_t are the solubility of CUR in the absence and presence of CD, respectively.

Determination of Job plot

Confirmation of stoichiometry of inclusion complexes was by Job plot. Job plot also known as the continuous variation method or Job's method involves determination of binding stoichiometry of CUR and cyclodextrin [25–27]. Briefly, added equimolar (10×10^{-6} M) solutions of CUR to CD (with α -CD, β -CD and γ -CD) solutions individually in varying ratios (1:9, 2:8, 3:7 and so on) of drug and CD to make 10 ml, keeping the total concentration of solutes constant. In addition, prepared an analogous set of CUR solutions without CDs in distilled water. Finally, absorbance of all the solutions was measured at 423 nm in Shimadzu UV-1700 PharmaSpec UV-Vis spectrophotometer (Shimadzu, Japan). The difference in absorbance of CUR in the presence and in absence of CD was plotted against R where R is obtained by the following equation:

$$R = \frac{[\text{CUR}]}{[\text{CUR}] + [\text{CD}]} \quad (4)$$

where [CUR] and [CD] are concentrations of curcumin and cyclodextrin, respectively.

All the determinations were conducted in triplicate.

In silico molecular modelling studies

Investigated in silico molecular modelling and docking study to study the ease with which CUR complexes with α -CD, β -CD and γ -CD. Calculated the transition energies for docking CUR into each CD molecule. Firstly obtained crystal structures of α -, β - and γ CD (25YE, 2Y4S and 2ZyK) from protein data bank (PDB) and structures of α -, β - and γ CD was extracted [28, 29]. Performed molecular modeling studies in SYBYL7.1 installed on a silicon graphics fuel station. Manually docked CUR into α -, β - and γ CD by visualization and 3D tools of SYBYL7.1 and further minimized the structures by calculation of Powell's conjugate gradient. For all the four structures calculated Gasteiger-Hückel partial atomic charges by using over 1,000 iterations in order to ascertain the energy minimized conformations for each structure [30, 31]. After setting minimum energy difference of 0.005 kcal/mol as convergence criteria obtained CUR-CD complexes using tools in SYBYL7.1. [32, 33].

Computational studies for optimization of stability determination

Further optimized stability of each of the CUR-CD complex obtained from in silico studies. From PDB, downloaded complex crystal structures of α -, β - and γ CDs (25YE, 2Y4S and 2ZyK) and extracted α -, β - and γ cyclodextrin structures [28, 29]. Sketched and minimized the CUR molecule by Powell's conjugate gradient method and Tripos force field. Minimum energy difference of 0.001 kcal/mol was set as the convergence criteria. Applied Gasteiger-Hückel partial atomic charges for minimization of CUR and performed over 1,000 iterations to ascertain energy minimized conformations of each structure [30]. Subjected CUR-CD complexes to an optimization process by using GAUSSIAN 03 software package [34]. Performed complete optimizations by HF (Hartree-Fock) method with 3-21+G* and 6-31+G* basis set where Mulliken charges were used in the calculations. Computed frequencies of optimized species analytically to characterize each stationary point as a minimum or transition state and estimate the zero point vibrational energies (ZPE). The calculated ZPE values (at 298.15 K) were scaled by a factor of 0.9153 in the HF method. Calculated the energy of complex formation with respect to molecular form of CDs and CUR by the following equation:

$$E_{\text{complex}} = E_{\text{docked-complex}} - (E_{\text{curcumin}} + E_{\text{cyclodextrin}}) \quad (5)$$

Here,

E_{complex} = Energy of complex formation.

$E_{\text{docked-complex}}$ = Energy of optimized structure of docked-complex.

E_{curcumin} = Energy of optimized structure of curcumin.

$E_{\text{cyclodextrin}}$ = Energy of optimized structure of cyclodextrin.

Preparation of CUR-CD complexes by pulverization method

For preparation of CUR-CD complexes equimolar ratios (1:1) of CUR and the CDs (5 of CUR, 13.2 of α -CD, 15.25 of β -CD and 17.6 gm of γ -CD) were weighed. Triturated individually CUR and CD and mixed thoroughly (30 min) to form CUR-CD complex. Characterized and evaluated the CUR-CD complexes.

Evaluation studies of CUR-CD complex

Curcumin content

The CUR content was estimated in CUR-CD complexes by HPLC at 423 nm. Briefly, dissolved in methanol (40 %

v/v), sample containing 10 mg of CUR/equivalent amount of CUR–CD complexes (36.4 of CUR α -CD, 40.5 of CUR β -CD and 55.2 mg of CUR γ -CD) for estimation. Estimation was carried out in triplicate.

Saturation solubility studies

Determined CUR and CUR–CD complexes solubility in three media: distilled water, SGF and FaSSIF. Dissolved excess amount of CUR/CUR–CD complexes in water (5 ml) in Schott Duran bottles subjected to constant shaking in Water Bath Shaker (Model RSB-12, REMI Laboratory Instruments, India) for 2 h at 37 °C. Estimated CUR dissolved by HPLC at 423 nm after filtration of samples and suitable dilution with methanol (40 % v/v). The solubility study was conducted in triplicate.

Dissolution studies

The in vitro dissolution study of CUR (100 mg) and CUR–CD complexes (~100 mg) were in USP Dissolution Test apparatus type II (Electrolab TDT-06P, India). Dissolution study was for 2 h in SGF (900 ml) and 10 h in FaSSIF (900 ml) at 75 rpm stirring speed at 37° \pm 0.5 °C. Sampled (5 ml) at time intervals of 0.25, 0.5, 0.75, 1, 1.5, 2, 2.5, 4, 8, and 12 h. Estimated CUR dissolved by HPLC at 423 nm after filtration and suitable dilution of samples. The in vitro dissolution studies were conducted in triplicate.

Fourier-transform infrared spectra (FTIR)

Fourier-transform infrared spectra (FTIR) of CUR, CDs and CUR–CD complexes were recorded in Perkin Elmer Spectrum BX infrared spectrophotometer. Samples were thoroughly mixed with dry KBr and compressed under high pressure to obtain transparent discs. Placed the disc in sample holder of IR spectrophotometer and scanned the spectrum range from 4,000–400 cm^{-1} .

Differential scanning calorimetry (DSC)

The thermal behaviour of CUR, CDs and CUR–CD complexes were examined by DSC using Mettler–Toledo DSC module controlled by Star software (Mettler–Toledo GmbH, Switzerland). Samples were weighed (5.00–8.00 mg) and placed in sealed aluminium pans. DSC analysis was carried out at a heating rate of 10 °C/min under flow of nitrogen. The observations were recorded over a temperature range of 40–400 °C.

Powder X-ray diffraction studies (PXRD)

Powder X-ray diffraction (PXRD) of CUR, CDs and CUR–CD complexes were determined using a PAN Analytical

X'pert PRO diffractometer (The Netherlands) equipped with a rotating target X-ray tube and wide-angle goniometry. The X-ray source was $\text{K}\alpha$ radiation from a copper target ($\lambda = 1.5418$). The X-ray tube was operated at a potential of 40 kV and a current of 30 mA. The range (2θ) of the scans was from 0° to 50° and the scan speed was maintained at a rate of 2° per minute and increased at increments of 0.02°.

Nuclear magnetic resonance (NMR) studies

The ^1H -NMR spectra was recorded on a BRUKER AVANCE 11 400 MHz spectrometer at 298 K. CUR was dissolved in DMSO while pure CDs and CUR–CD complexes were dissolved in deuterated water (D_2O). ^1H -NMR chemical shift measured in δ parts per million (δ ppm) caused upon complexation were measured to determine inclusion of CUR in the CDs. Processing and analysis of the data was performed with MestReNova-Software (Mestrelab Research S.L., Version 6.1.1).

In vivo bioavailability study

The in vivo bioavailability studies of CUR and CUR–CD complexes in Male New Zealand rabbits (1.5–2.5 kg from Biogen Laboratory, Bangalore). Animals were maintained under standard laboratory conditions. (20–25 °C, 50 \pm 5 % RH; 12 h light/12 h dark cycle) and allowed access food and water ad libitum. All experiments were performed in accordance to the guidelines of committee for control and supervision of experiments on animal (CPC-SEA), Ministry of Culture, and Government of India with approval from the Institutional Animal Ethics Committee.

Formed four groups containing three rabbits randomly assigned in each group for the bioavailability study. The animals were fasted overnight before the experiment with free access to water. Orally administered CUR (1 gm/kg) and CUR–CD complexes (~1 gm/kg of CUR) in water to different groups of animals. Group I received pure CUR while Group II received CUR α -CD, Group III received CUR β -CD and Group IV received CUR γ -CD. Blood samples (1 ml) were collected from the marginal ear vein of animals into heparinized tubes at time intervals of 0, 5, 10, 15, 20, 25, 30 and 60 min after administration. Preliminary studies indicated plasma concentration of pure CUR was below the minimum detectable level after 60 min while it was detectable for longer duration in CUR–CD groups. Blood samples were therefore collected from CUR–CD administered groups at 0, 0.25, 0.5, 0.75, 1, 1.5, 2, 4, 8, 12 and 24 h after administration. Blood samples were centrifuged at 12,000 rpm for 10 min to obtain plasma. Mixed the plasma aliquots (0.5 ml) with 2,000 units of β -glucuronidase in 0.1 M sodium phosphate buffer

(pH 6.8) and β -sulfatase solution in 0.1 M sodium acetate buffer (pH 6.5) and incubated at 37 °C for 1 h. Acidified the obtained solution with 50 μ l of 1 M glacial acetic acid and thoroughly mixed in cyclomixer (REMI Laboratory instruments, India). Added 50 μ l of quercetin (internal standard) and 1 ml of acetonitrile to the solution and centrifuged at 1,000 rpm for 10 min. Analyzed by HPLC at 423 nm and quantified the amount of CUR present in the supernatant. Selected Hibar C18 column (150 \times 4.6 mm) packed with 5 μ m particles while the mobile phase consisted of acetonitrile, tetrahydrofuran and 2 % acetic acid mixture in 50:5:45 ratios.

Development of bio-analytical method for estimation of curcumin

Prepared individually stock standard solutions of CUR (200 μ g/ml) and quercetin (internal standard, IS, 6 mg/ml) in methanol. Prepared five concentrations of standard CUR solutions (0.1–5 μ g/ml) from the CUR stock solution for standard calibration curve. For the bio-analytical method, acidified rabbit plasma (900 μ l) with 1 M glacial acetic acid (50 μ l), added CUR (50 μ l) and thoroughly mixed. Spiked the resultant solution (500 μ l) with 50 μ l of IS and mixed thoroughly. Added Acetonitrile (1 ml) to precipitate proteins mixed thoroughly and centrifuged for 10 min at 1,000 rpm. Analyzed by HPLC at 423 nm and quantified the amount of CUR present in the supernatant. In 0.1–5 μ g/ml concentration range the calibration curve was linear for CUR was linear. Determined by Kinetica software (Thermo Scientific) the following pharmacokinetic parameters: area under the curve AUC_{0-t} , total area under the curve ($AUC_{0-\infty}$) (μ g/ml h), terminal phase half-life ($t_{1/2}$) (h), peak plasma concentration (C_{max}) (μ g/ml), time to reach the maximum plasma concentration (t_{max}), elimination rate constant K_e (h^{-1}), and mean retention time MRT (h). Relative bioavailability (F) of CUR–CD complexes were calculated from the following equation:

$$F = 100 \times \frac{[AUC_A \times D_B]}{[AUC_B \times D_A]} \quad (6)$$

where F is relative bioavailability; AUC_A is area under curve of curcumin; AUC_B is area under curve of cyclodextrin; D_A is dose of curcumin and D_B is dose of cyclodextrin.

Statistical analysis

Non-compartment model analysis of pharmacokinetic plasma concentration–time data was by Kinetica software (Thermo Scientific). Pharmacokinetic parameters determined include area under AUC_{0-t} , the curve total area under the curve ($AUC_{0-\infty}$), terminal phase half-life ($t_{1/2}$),

peak plasma concentration (C_{max}) and time to reach the maximum plasma concentration (T_{max}), elimination rate constant K_e , and mean retention time MRT.

All the results were expressed as mean \pm standard deviation (SD). Statistical analysis of $AUC_{0-\infty}$ was performed with GraphPad Prism (Demo version) by one-way ANOVA and Dunnett's post hoc test for multiple comparisons. $p < 0.05$ was considered as statistically significant difference.

In vitro–in vivo correlation

Computed IVIVC Level A correlation for CUR and CUR–CD complexes by linear regression analysis of a plot of percentage drug dissolved in vitro and percentage drug absorbed. Determined by Wagner–Nelson method the percentage of drug absorbed from the CUR plasma concentration versus time data [35].

Results and discussion

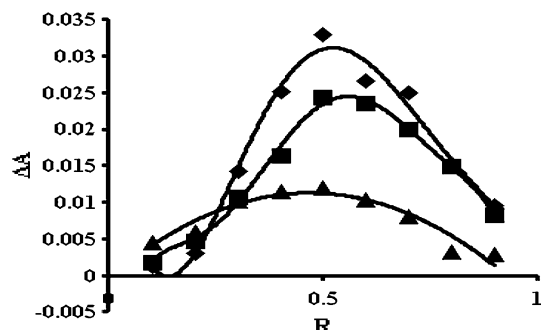
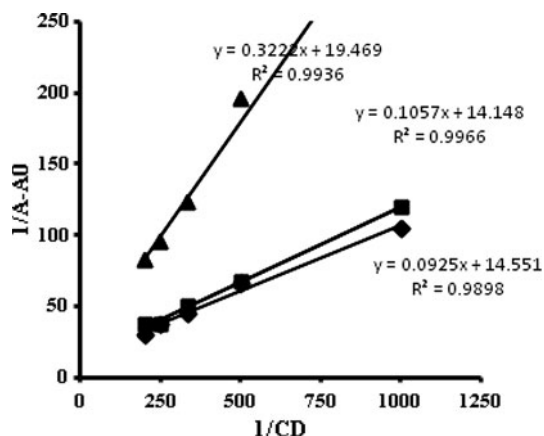
Phase-solubility studies

Figure 1 presents the phase-solubility diagrams for CUR with α -CD/ β -CD/ γ -CD binary systems. A linear increase was observed in the aqueous solubility of CUR with an increasing concentration of CD. This is indicative of A_L type solubility diagram where stoichiometry of CUR–CD is 1:1 which was further confirmed by slope < 1 in the solubility diagrams [26]. Calculated apparent stability constant, K_s , of CUR–CD complexes from Eq. 2 and observed K_s of α -CD complex $>$ γ -CD complex $>$ β -CD complex (Table 1). Considerable high K_s observed in α -CD complex indicates its increased stability in comparison to γ -CD complex and β -CD complex. Further, confirmed stoichiometry of CUR–CD complexes by Job's plot (Fig. 2) and double-reciprocal plots (Fig. 3). In Job's plot obtained R value of 0.5 and observed a linear relationship when $1/(A-A_0)$ was plotted against $1/CD$ ($R^2 = 0.9898, 0.9966$ and 0.9936 for CUR α -CD, CUR β -CD and CUR γ -CD respectively).

The driving force for inclusion complexation between CD and CUR includes van der Waals interaction, hydrogen bonding, and hydrophobic interaction which results in the release of high-energy water molecules from CD cavity and release of strain energy from the CD ring. The optimum apparent stability constant K_s for enhancement in solubility and stability of poorly soluble drug molecules lies between 200 and 5,000 M^{-1} [36]. The K_s values of CUR–CD complexes were all in the range of 559–1,125 M^{-1} indicating the capability of complexes in improving the solubility and stability of CUR with α -CD $>$ γ -CD $>$ β -CD.

Table 1 Stability constant of complexes of curcumin

Type of cyclodextrin	Stability constant (K_s ; M^{-1})
α CD	1,124.606 ($r^2 = 0.9859$)
β CD	558.909 ($r^2 = 0.9845$)
γ CD	746.714 ($r^2 = 0.9710$)

**Fig. 2** Job's plot of curcumin cyclodextrin complexes filled diamond alpha CD, filled square beta CD, filled triangle gamma CD**Fig. 3** Dependence of curcumin cyclodextrin complex absorbance on cyclodextrin concentrations filled diamond alpha CD, filled square beta CD, filled triangle gamma CD

Gibbs-free energy is a thermodynamic function. Change in Gibbs-free energy (ΔG°) is the net energy available to do useful work and is a measure of “free energy”. Negative ΔG° indicates a spontaneous process [36]. Table 2 presents ΔG° obtained by substituting solubility of CUR in presence and absence of CD in Eq. 3. ΔG° values were negative which increased with an increase in CD concentration. Hence CD solution is a more favourable environment than water for CUR molecule and order of spontaneity of α -CD complex > γ -CD complex > β -CD complex.

In silico molecular modelling studies

Figure 4 presents structures of CUR-CD complexes from molecular modelling studies. The energy values obtained

Table 2 Gibbs free energy data of Curcumin-CD complex in water

Concentration of CD (mM)	Gibb's free energy ($-\Delta_{\text{trans}}G^\circ/\text{cal mol}^{-1}$)		
	α CD	β CD	γ CD
2.5	421.863	296.749	357.691
5	556.697	356.143	416.051
7.5	610.095	461.893	492.632
10	683.037	511.535	590.683

of CUR α -CD complex (130.5) < CUR β -CD complex (145.6) < CUR γ -CD complex (171.2 kcal/mol). Based on the energy values most favoured complex is CUR α -CD complex. Table 3 presents the data of optimization studies. Based on the energy of complex formation, CUR α -CD and CUR β -CD complexes are more stable than CUR γ -CD complex by hf/6-31G* level of calculations. However, when hf/3-21G* is adopted, CUR β -CD is less stable than CUR α -CD and CUR γ -CD complexes. Considering that hf/6-31G* level of calculations are more accurate than hf/3-21G*, stability of CUR α -CD and CUR β -CD complexes may be more than CUR γ -CD complex.

Evaluation of curcumin cyclodextrin complexes

Evaluated spray drying, pH modified method (procedure not provided in the text) in the preparation of CUR-CD complexes. However, CUR degraded in the presence of water. Hence, pulverization or co-grinding technique was selected for the preparation of CUR-CD complexes. Pulverization ensured stability of CUR and can be easily scaled-up.

Figure 5 presents aqueous solubility of CUR-CD complexes expressed in mg/ml. Observed considerable improvement in solubility of CUR in all the CD complexes with α -CD complex > β -CD complex > γ -CD complex. In comparison to pure CUR (0.002 mg/ml) α -CD complex (0.364 mg/ml) had almost 135-fold increase in solubility while β -CD complexes (0.186 mg/ml) exhibited 69-fold increase and γ -CD (0.068 mg/ml) exhibited 25-fold increase in solubility. In our earlier studies observed enhanced in solubility of CUR in hydroxy propyl β -CD (HP β CD) and methyl β -CD (M β CD) [22]. Increased solubility of CUR is due to decrease in crystallinity of CUR in CUR-CD complexes during pulverization and increased wetting [37].

Dissolution study

In Fig. 6 presented CUR and CUR-CD complexes dissolution profiles in SGF and FaSSIF. Observed an enhanced dissolution in all the CUR-CD complexes as shown by the

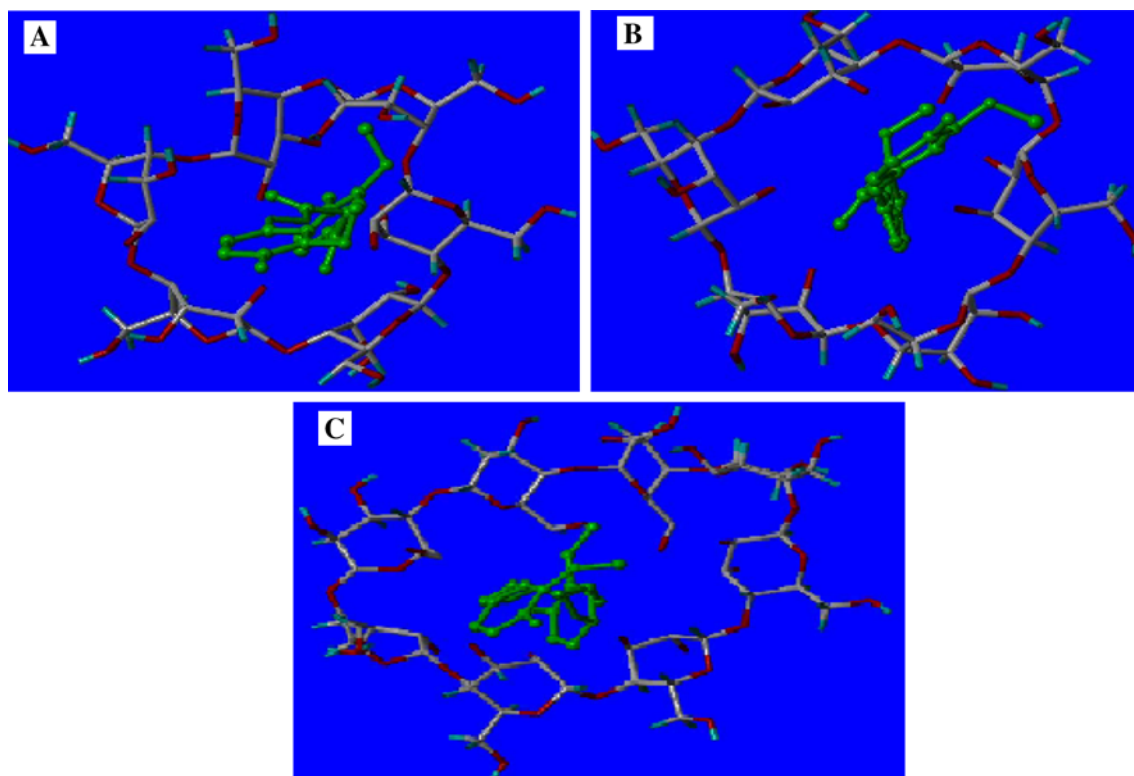


Fig. 4 In silico molecular modelling structures of **A** CUR α -CD complex **B** CUR β -CD complex **C** CUR γ -CD complex

Table 3 Calculation of energy of CUR-CD complex formation by Hartree-Fock Method

Particulars	E_{hf}	ZPC	E_{corr}	E_{complex}
hf/3-21G*				
CUR	–	0.4	–783,274.30	
Alp	–	1.21	–2,273,254.46	–21.51
Beta	–	1.31	–2,605,484.87	–30.41
Gam	–	1.49	–2,984,364.74	–23.28
Acid	–	1.65	–3,056,801.98	
Bcd	–	1.71	–3,389,041.29	
Gcd	–	1.89	–3,767,914.03	
hf/6-31G*				
CUR	–	0.40	–787,590.30	
Alp	–	1.12	–2,284,924.62	–23.51
Beta	–	1.31	–2,618,784.47	–22.52
Gam	–	1.49	–2,999,608.71	–06.99
Acid	–	1.53	–3,072,538.43	
Bcd	–	1.71	–3,406,397.29	
Gcd	–	1.90	–3,787,206.00	

CUR curcumin, Alp α -CD, Beta β -CD, Gam γ -CD, Acid CUR α -CD complex, Bcd CUR β -CD complex, Gcd CUR γ CD complex, E_{hf} is absolute energy values calculated in Hartree, ZPC is the zero point correction energy, E_{corr} is corrected energy in kcal/mol after zero point energy correction process E_{complex} is the energy of complex formation in kcal/mole

time taken for 50 % CUR release. At the end of 2 h, the extent of dissolution in SGF was 13.24, 77.18, 69.4 and 45.33 % from CUR, CUR α -CD complex, β -CD complex and γ -CD complex, respectively. The extent of dissolution at the end of 12 h in FaSSIF were 14.53, 91.84, 83.89 and 60.28 % from CUR, CUR α -CD, CUR β -CD and CUR γ -CD complexes, respectively. This observed increase in the dissolution of CUR may be due to formation of readily soluble complexes because of increased wettability of complexes. Enhancement in dissolution was maximum in CUR α -CD followed by CUR β -CD and CUR γ -CD. Compounds with aliphatic chains form inclusion complexes with α -CD because of its small cavity size while compounds with aromatic rings, exemplified by paclitaxel, form complexes with β -CD [38]. Consequently, CUR may form inclusion complexes to a greater extent in α -CD than in β -CD or γ -CD because of its low molecular weight (354.49).

Characterization of CUR-CD complexes

CUR-CD complexes were characterized by various spectroscopy techniques. FTIR spectrum was recorded to analyse the structure of CUR-CD complex and determine occurrence of any chemical change in the complex (Fig. 7).

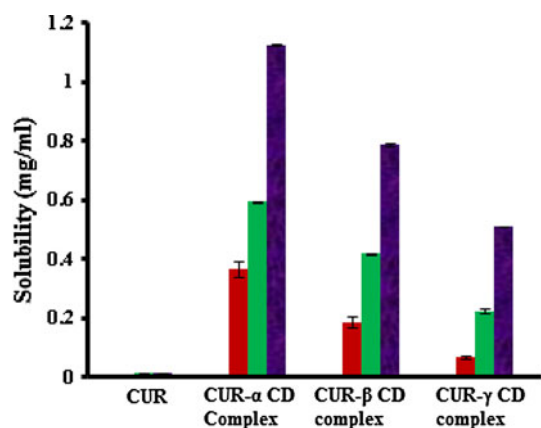


Fig. 5 Solubility of curcumin and CUR-CD complexes in distilled water, simulated gastric fluid (SGF) and fasted state simulated intestinal fluid (FaSSIF) Mean \pm SD, $n = 3$; red filled square Distilled water, green filled square SGF pH1.2, violet filled square FaSSIF

In the FTIR spectra, the characteristic peaks of CUR appear at 3,664.97 corresponding to phenolic (OH) vibrations; 3,014.33 corresponding to aromatic C-H stretching vibrations; 1,602 cm^{-1} corresponding to the stretching vibration of the benzene ring skeleton, 1,510.68 to the mixed (C=O) and (C=C) vibration; 1,272.85 cm^{-1} to enol C-O peak; and 1,023 cm^{-1} to C-O-C peak [39]. A sharp peak of hydroxyl (—OH) group at 3,510.20 cm^{-1} indicates the presence of free hydroxyl (—OH) group. Observed no change in IR spectra of CUR-CD complexes except for broadening of the hydroxyl group peak at 3,379.05 cm^{-1} , which may suggest occurrence of interaction of the hydroxyl (—OH) group. The bands within the range of 3,079–3,000 cm^{-1} were observed, which can be attributed to aromatic C-H stretching vibration, indicating possible intercalation of CUR in CD complex.

DSC has been extensively adopted to evaluate thermal properties of cyclodextrin complexes. It has the potential to provide qualitative and quantitative information regarding the physicochemical state of CUR inside the CD complexes. In general, complexation results in the absence of endothermic peak or shift of peak to different temperature because of change in the initial crystal lattice, melting, boiling or sublimation points. In the present study, as observed in Fig. 8, DSC thermogram of CUR had a sharp endothermic characteristic peak at 150 °C. Thermograms of pure α -CD and β -CD had two peaks, one peak at about 60 °C and another peak at around 300 °C while the thermogram of pure γ -CD had a peak at 300 °C. DSC thermograms of CUR-CD complexes exhibited a pattern of reduction in the sharp endothermic peak of CUR with slight broadening without any change in temperature. Further, observed in α -CD complex and β -CD complex a similar broadening of peak at around 60 °C with a slight shift in temperature of the second endotherm at 300 °C.

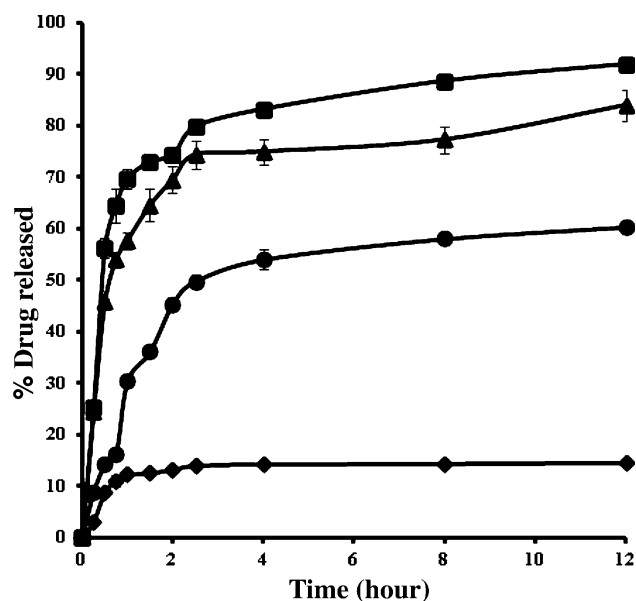


Fig. 6 Dissolution profiles of curcumin and CUR-CD complex. Mean \pm SD, $n = 3$; filled diamond Pure drug, filled square CUR- α CD complex, filled triangle CUR- β CD complex, filled circle CUR- γ CD complex

Similarly, observed a slight shift in the endothermic peak at 300 °C in γ -CD complex. This phenomenon is indicative of interaction between CUR and CDs. From the area of endothermic peak obtained the extent of complexation of CUR in CD complexes with β -CD complex (82 %) > γ -CD complex (71 %) > α -CD complex (65 %).

In P-XRD studies, presented in Fig. 9, CUR has two intense peaks at 9.0485 and 17.4957 degrees apart from other characteristic peaks which indicate its crystalline nature. Pure α -CD has intense peaks at 11.9508, 12.2235, 13.5856, 14.3873 and 21.7351 degrees. Similarly, pure β -CD has intense peaks at 9.1595 and 12.7292; however pure γ -CD is amorphous, with decreased intensity of peaks in comparison to α -CD and β -CD. All the CUR-CD complexes exhibited a decrease in intensity of peaks when compared to pure CUR and pure CDs indicating a decrease in the crystallinity of CUR in CD complexes. This decrease in CUR crystallinity is responsible for increased solubility of CUR in all the CD complexes.

NMR spectroscopy may provide a direct evidence of inclusion complex formation. An overview of ^1H -NMR chemical shifts of hydrogen atoms of cyclodextrin in D_2O the complexation induced chemical shifts in their respective complexes is presented in Table 4. In α -CD complexes, maximum involvement appears to be H_1 hydrogen followed by H_5 hydrogen. In CUR β -CD complex maximum involvement is of H_1 and H_3 hydrogen. In γ -CD complex there is involvement of H_1 , H_2 , H_4 and H_5 hydrogen atoms. Among the CD complexes, in α -CD complexes the involvement of hydrogen atoms of CD appears to be the

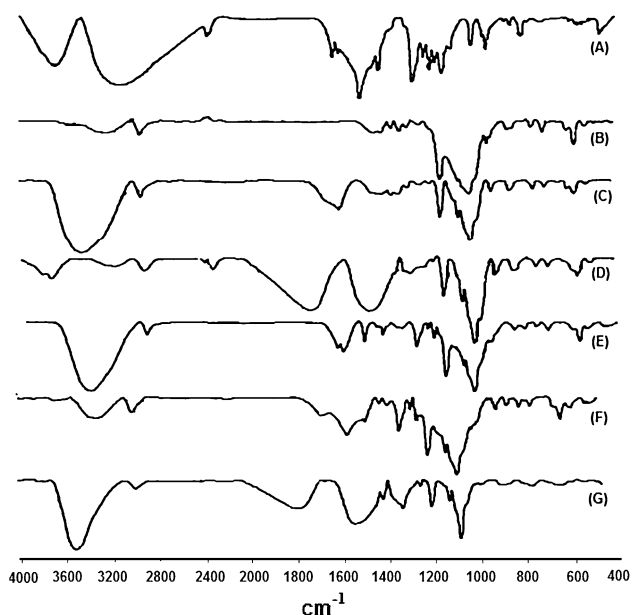


Fig. 7 FTIR Spectra of A CUR, B Pure α -CD, C Pure β -CD, D Pure γ -CD, E CUR α -CD complex, F CUR β -CD complex and G CUR γ -CD complex

least. All the CD complexes exhibited involvement of H₃ or H₅ hydrogen atoms which is normally expected in cyclodextrin complexation. In addition they exhibited involvement of H₁, H₂, H₄ hydrogen atoms. This phenomenon may be explained by the pulverization technique adopted in the preparation of CUR-CD complex Table 5.

In vivo bioavailability studies

Figure 10 illustrates CUR plasma concentration profiles from pure CUR and CUR-CD complexes. Table 5 summarizes the pharmacokinetic parameters obtained from one compartmental analysis of experimental data by Kinetica 2000 software (Thermo Scientific). CUR-CD complexes exhibited an increase in $t_{1/2}$, t_{max} , C_{max} , AUC, K_a , and MRT; and decrease in K_e , clearance and V_d . Statistically analyzed AUC_{0-∞} values by one-way analysis of variance (ANOVA) and Dunnett's post hoc test for multiple comparisons. CUR-CD complexes exhibited significant ($p < 0.05$) enhanced AUC in comparison with CUR. Increase in AUC of CUR α -CD complex (3.88 $\mu\text{g/ml h}$) > CUR β -CD complex (3.149 $\mu\text{g/ml h}$) > CUR γ -CD complex (0.801 $\mu\text{g/ml h}$).

There is a significant difference ($p < 0.05$) in the AUC of CUR α -CD complex and CUR γ -CD complex. However, there is no significant difference between CUR α -CD and CUR β -CD complexes. To summarize, observed an increase in the AUC of CUR α -CD complex > CUR β -CD complex > CUR γ -CD complex. Relative bioavailability

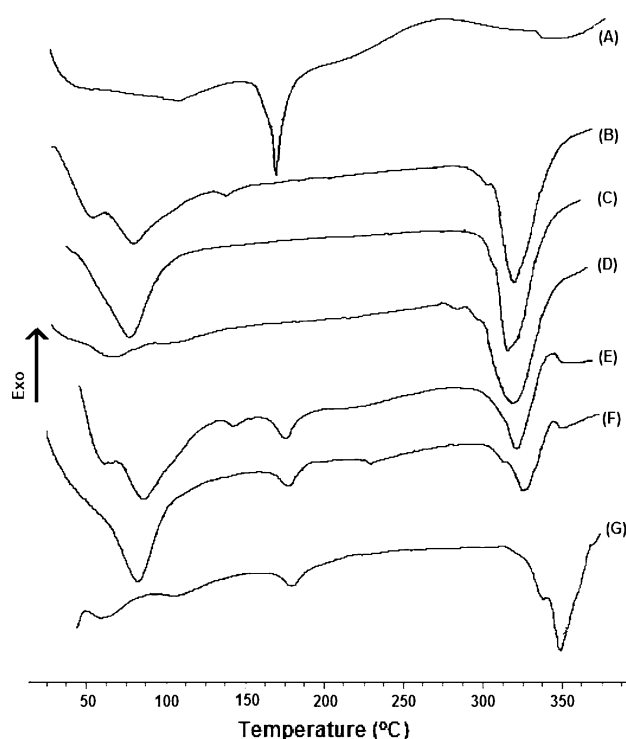


Fig. 8 DSC thermograms of pure drug and complexes of A CUR, B Pure α -CD, C Pure β -CD, D Pure γ -CD, E CUR α -CD complex, F CUR β -CD complex, and G CUR γ -CD complex

of CUR α -CD, CUR β -CD and CUR γ -CD complexes were 460, 365 and 99 % with reference to pure CUR.

Increase in bioavailability exhibited by CUR α -CD complex can be attributed to the observed increase in inclusion of CUR in α -CD. Increase in CUR solubility in CUR-CD complexes may decrease the extent of its pre-systemic and systemic metabolism because of enzyme saturation at the site of metabolism. This phenomenon can increase the amount of CUR available for absorption and systemic circulation resulting in enhanced bioavailability of CUR in the CD complexes. Reports of enhanced CUR solubility and bioavailability from curcumin-phospholipid complex are available in the literature. One study reported 5-fold increase CUR oral bioavailability from CUR formulation with phosphatidyl choline (Meriva) [19]. Another study reported 3-fold increase in CUR aqueous solubility with increased hepatic protective action [40]. Reports of enhancement in solubility and bioavailability of drugs with poor solubility undergoing pre-systemic and systemic metabolism are available in the literature. For instance, raloxifene exhibits poor absolute oral bioavailability ($\sim 2\%$) attributed to its extensive first-pass metabolism by glucuronidation and poor aqueous solubility [38]. Wempe et al. reported a two-fold increase in C_{max} and a 3-fold increase in raloxifene AUC from raloxifene-hydroxybutenyl-beta cyclodextrin complex in male Wistar-Hanover rats [41, 42].

Fig. 9 X-ray diffraction patterns of *A* CUR, *B* pure α -CD, *C* pure β -CD, *D* pure γ -CD, *E* CUR α -CD complex, *F* CUR β -CD complex and *G* CUR γ -CD complex

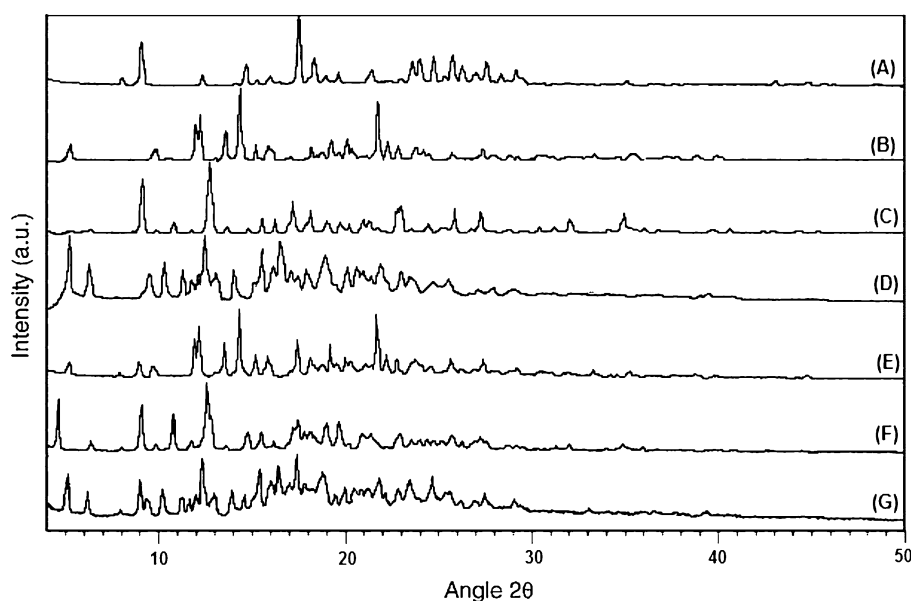


Table 4 ^1H -NMR chemical shifts of cyclodextrin hydrogen atoms in D_2O and their complexation induced chemical shifts in their respective complexes

Hydrogen	α -CD Δ	CUR α -CD δ (Δ δ)	β -CD δ	CUR β -CD δ (Δ δ)	γ -CD δ	CUR γ -CD δ (Δ δ)
1	4.96	4.92 (0.04)	4.91	5.00 (0.09)	5.07	4.96 (1.01)
2	4.72	4.69 (0.03)	4.64	4.69 (0.05)	4.80	4.69 (1.11)
3	3.86	3.84 (0.02)	3.78	3.87 (0.09)	3.89	3.84 (0.05)
4	3.76	3.74 (0.02)	3.71	3.72 (0.01)	3.84	3.75 (0.09)
5	3.51	3.48 (0.03)	3.46	3.44 (0.02)	3.60	3.50 (1.00)

Table 5 Pharmacokinetic data of CUR and CUR-CD Complex

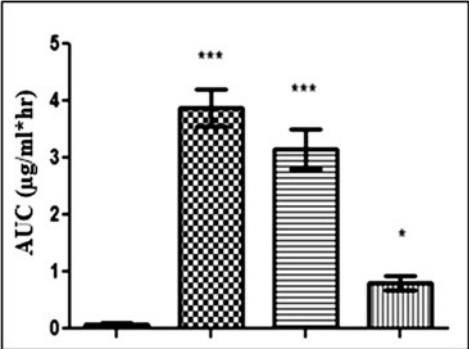
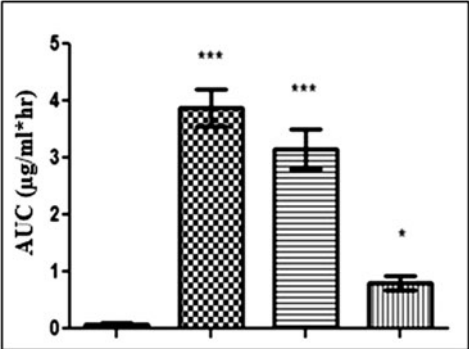
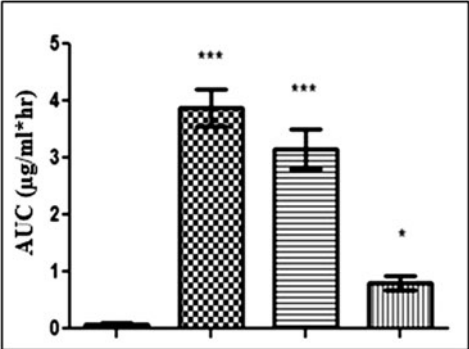
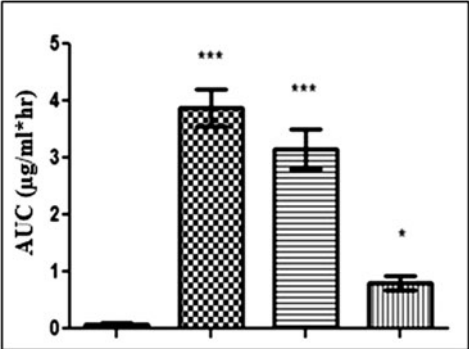
Parameters	CUR	CUR- α CD Complex	CUR- β CD Complex	CUR- γ CD Complex
AUC_{0-n} ($\mu\text{g/ml h}$)	0.072 ± 0.01	3.438 ± 0.24	2.525 ± 0.097	0.684 ± 0.045
AUC_{tot} ($\mu\text{g/ml h}$)	0.089 ± 0.01	3.879 ± 0.33	3.149 ± 0.35	0.801 ± 0.13
K_e (h^{-1})	1.88 ± 0.12	0.289 ± 0.02	0.146 ± 0.036	0.290 ± 0.11
K_a (h^{-1})	2.303 ± 0.02	5.174 ± 0.25	2.64 ± 0.26	1.289 ± 0.14
$\text{T}_{1/2}$ (h)	0.369 ± 0.02	2.396 ± 0.16	4.940 ± 1.314	2.631 ± 1.03
MRT (h)	0.561 ± 0.03	4.255 ± 0.14	7.52 ± 1.56	4.320 ± 1.32
Clearance (ml h^{-1})	$11,301.89 \pm 1,076$	259 ± 23.07	320 ± 36.37	$1,271 \pm 219.37$
Vd (ml)	$6,023.03 \pm 64.13$	896 ± 22.87	$2,241 \pm 356.44$	$4,646.67 \pm 1,046.39$

There is a correlation between pharmacokinetic and computation data. Energy values from molecular docking indicate CUR α -CD complex < CUR β -CD complex < CUR γ -CD complex. Similarly, computational studies and from Gibbs-free energy values indicate CUR α -CD complex to be most stable CD complex. The stability of CUR β -CD complex > CUR γ -CD complex from the computational studies; while stability of CUR γ -CD

complex > CUR β -CD from apparent (K_s) and Gibbs-free energy (ΔG°) values.

In vitro–in vivo correlation (IVIVC)

In the present study attempted prediction of Level A correlation. Plotted percentage of CUR absorbed versus percentage of CUR dissolved from CUR-CD complexes

Fig. 10 Plasma concentration–time profile of CUR and CUR cyclodextrin complexes. Mean \pm SD, $n = 6$ Pure drug, filled pink square CUR- α CD complex, filled brown diamond CUR- β CD complex, filled violet circle CUR- γ CD complex; Inset Fig.  Pure drug,  CUR- α CD complex,  CUR- β CD complex,  CUR- γ CD complex. Values of *** $p < 0.001$; * $p < 0.1$

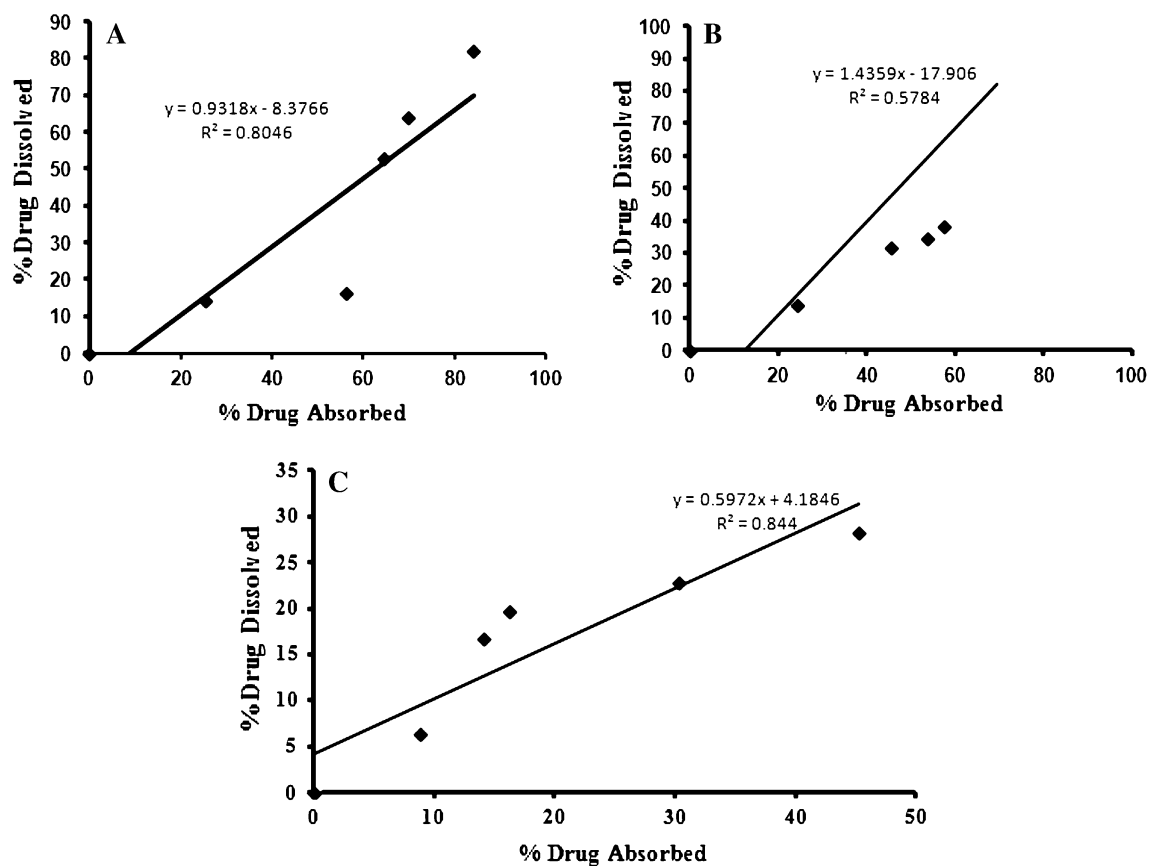
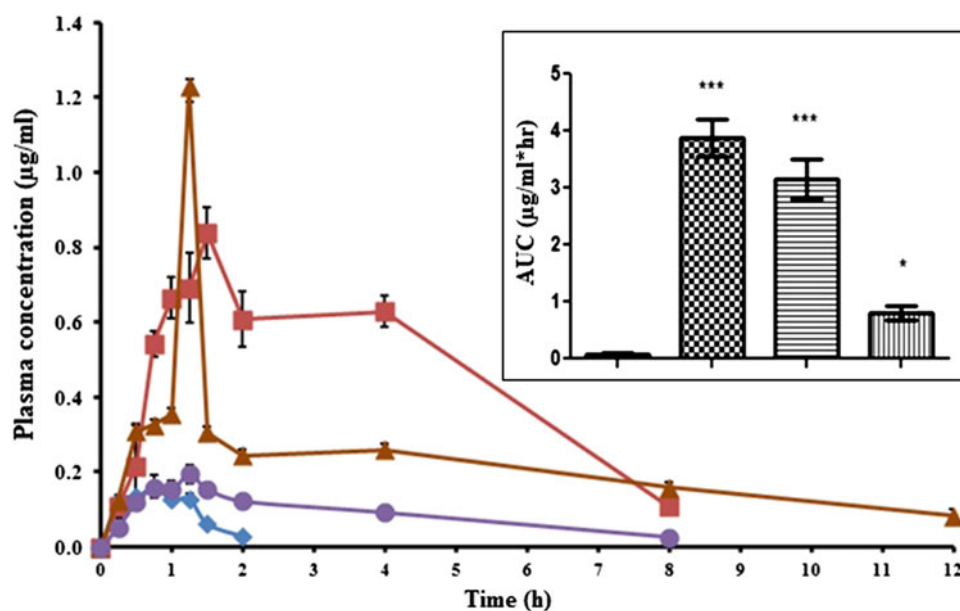


Fig. 11 In vitro-in vivo correlation of percentage drug absorbed and percentage drug released of **A** CUR α -CD complex, **B** CUR β -CD complex and **C** CUR γ -CD complex

(Fig. 11). From the correlation plots obtained regression coefficient (R^2) of 0.805, 0.578 and 0.844 for CUR α -CD, CUR β -CD and CUR γ -CD complexes, respectively. On

the contrary, obtained no correlation plot from pure CUR which may be explained by its inherent poor solubility and permeability considering it is a BCS Class IV drug.

IVIVC has gained considerable significance because of it can be successfully applied to predict in vivo performance from in vitro behavior [43]. Among the four levels of IVIVC, Level A is considered to be the highest level of correlation which aims to predict the entire in vivo concentration time course from the in vitro dissolution profile. Prediction of Level A correlation essentially involves evaluation of point-to-point correlation between in vitro and in vivo profiles [44].

In conclusion, observed altered IVIVC behaviour by inclusion complexation of CUR with CUR α -CD complex and CUR γ -CD exhibiting greater correlation than CUR β -CD complex. Altered IVIVC behaviour has been observed in pioglitazone, a BCS Class 2 drug, where increase in drug solubility leads to better correlation between in vitro and in vivo profiles [45].

Conclusions

From ancient times in Ayurveda turmeric has been used in treating a number of ailments. Curcumin the active principle of turmeric has poor aqueous solubility and oral bioavailability which precludes its use in therapy. In this study investigated the effect of curcumin-CD complexation on its solubility and bioavailability. Pulverization method resulted in significant enhancement of CUR solubility with CUR α -CD complex > CUR β -CD complex > CUR γ -CD complex. Gibbs-free energy and in silico molecular docking studies favour formation of α -CD complex > β -CD complex > γ -CD complex. Maximum enhancement in dissolution and bioavailability of curcumin was observed from CUR α -CD complex. Enhanced relative bioavailability was observed in all CUR-CD complexes with CUR α -CD complex > CUR β -CD complex > CUR γ -CD complex.

Acknowledgments Authors would like to thank Prof. B.G. Shivananda, Principal, Al-Ameen College of Pharmacy for his kind support and encouragement to carry out this project.

References

- Aggarwal, B.B., Sundaram, C., Malani, N., Ichikawa, H.: Curcumin: the Indian solid gold. *Adv. Exp. Med. Biol.* **595**, 1–75 (2007)
- Huang, H.C., Jan, T.R., Yeh, S.F.: Inhibitory effect of curcumin, an anti-inflammatory agent, on vascular smooth muscle cell proliferation. *Eur. J. Pharmacol.* **221**, 381–384 (1992)
- Lim, G.P., Chu, T., Yang, F., Beech, W., Frautschy, S.A., Cole, G.M.: The curry spice curcumin reduces oxidative damage and amyloid pathology in an Alzheimer transgenic mouse. *J. Neurosci.* **21**, 8370–8377 (2001)
- Natarajan, C., Bright, J.J.: Curcumin inhibits experimental allergic encephalomyelitis by blocking IL-12 signalling through Janus kinase-STAT pathway in T lymphocytes. *J. Immunol.* **168**, 6506–6513 (2002)
- Mazumder, A., Neamati, N., Sunder, S., Schulz, J., Pertz, H., Eich, E., Pommier, Y.: Curcumin analogs with altered potencies against HIV-1 integrase as probes for biochemical mechanisms of drug action. *J. Med. Chem.* **40**, 3057–3063 (1997)
- Awasthi, S., Srivastava, S.K., Piper, J.T., Singhal, S.S., Chaubey, M., Awasthi, Y.C.: Curcumin protects against 4-hydroxy-2-trans-nonenal-induced cataract formation in rat lenses. *Am. J. Clin. Nutr.* **64**, 761–766 (1996)
- Ukil, A., Maity, S., Karmakar, S., Datta, N., Vedasiromoni, J.R., Das, P.K.: Curcumin, the major component of food flavor turmeric, reduces mucosal injury in trinitrobenzene sulphonic acid-induced colitis. *Br. J. Pharmacol.* **139**, 209–218 (2005)
- Aggarwal, B.B., Kumar, A., Bharti, A.C.: Anticancer potential of curcumin: preclinical and clinical studies. *Anticancer Res.* **23**, 363–398 (2003)
- Mukhopadhyay, A., Bueso-Ramos, C., Chatterjee, D., Pantazis, P., Aggarwal, B.B.: Curcumin downregulates cell survival mechanisms in human prostate cancer cell lines. *Oncogene* **20**, 7597–7609 (2001)
- Shishodia, S., Potdar, P., Gairola, C.G., Aggarwal, B.B.: Curcumin (diferuloylmethane) down-regulates cigarette smoke-induced NF- κ B activation through inhibition of IkappaB α kinase in human lung epithelial cells: correlation with suppression of COX-2, MMP-9 and cyclin D1. *Carcinogenesis* **24**, 1269–1279 (2003)
- Mehta, K., Pantazis, P., McQueen, T., Aggarwal, B.B.: Anti-proliferative effect of curcumin (diferuloylmethane) against human breast tumor cell lines. *Anticancer Drugs* **8**, 470–481 (1997)
- Elattar, T.M., Virji, A.S.: The inhibitory effect of curcumin, genistein, quercetin and cisplatin on the growth of oral cancer cells in vitro. *Anticancer Res.* **20**, 1733–1738 (2000)
- Hanif, R., Qiao, L., Shiff, S.J., Rigas, B.: Curcumin, a natural plant phenolic food additive, inhibits cell proliferation and induces cell cycle changes in colon adenocarcinoma cell lines by a prostaglandin-independent pathway. *J. Lab. Clin. Med.* **130**, 576–584 (1997)
- Aggarwal, B.B., Swaroop, P., Protiva, P., Raj, S.V., Shirin, H., Holt, P.R.: Cox-2 is needed but not sufficient for apoptosis induced by Cox- selective inhibitors in colon cancer cells. *Apoptosis* **8**, 649–654 (2003)
- Thangapazham, R.L., Sharma, A., Maheshwari, R.K.: Multiple molecular targets in cancer chemoprevention by curcumin. *AAPS J.* **8**, E443–E449 (2006)
- Joe, B., Vijaykumar, M., Lokesh, B.R.: Biological properties of curcumin-cellular and molecular mechanisms of action. *Crit. Rev. Food Sci. Nutr.* **44**, 97–111 (2004)
- Yadav, V.R., Prasad, S., Kannappan, R., Ravindran, J., Chaturvedi, M.M., Vaahtera, L., Parkkinen, J., Aggarwal, B.B.: Cyclodextrin-complexed curcumin exhibits anti-inflammatory and antiproliferative activities superior to those of curcumin through higher cellular uptake. *Biochem. Pharmacol.* **80**, 1021–1032 (2010)
- Tonnesen, H.H., Masson, M., Loftsson, T.: Studies of curcumin and curcuminoids. XXVII. Cyclodextrin complexation: solubility, chemical and photochemical stability. *Int. J. Pharm.* **244**, 127–135 (2002)
- Anand, P., Kunnumakkara, A.B., Newman, R.A., Aggarwal, B.B.: Bioavailability of curcumin: problems and promises. *Mol. Pharm.* **4**, 807–818 (2007)
- Loftson, T., Brewster, M.E.: Pharmaceutical applications of cyclodextrins: 1. Drug solubilization and stabilization. *J. Pharm. Sci.* **85**, 1017–1025 (1996)
- Del Valle, Martin: E.M.: cyclodextrins and their uses: a review. *Process Biochem.* **39**, 1033–1046 (2004)
- Vivek, R.Y., Sarasija, S., Kshama, D., Seema, Y.: Effect of cyclodextrin complexation of curcumin on its solubility and

- antiangiogenic and anti-inflammatory activity in rat colitis model. *AAPS Pharm. Sci. Tech.* **10**, 752–762 (2009)
23. Wieslaw, M., Magdalena, Z.: Investigation of inclusion complex of trazodone hydrochloride with hydroxypropyl- β -cyclodextrin. *Carbohydr. Polym.* **77**, 482–488 (2009)
 24. Zopetti, G., Puppini, N., Pizzutti, M., Fini, A., Giovani, T., Comini, S.: Water soluble progesterone–hydroxypropyl- β -cyclodextrin complex for injectable formulations. *J. Incl. Phenom. Macrocycl. Chem.* **57**, 283–288 (2007)
 25. Swati, R., Sanjay, K.: Solubility enhancement of celecoxib using β -cyclodextrin inclusion complexes. *Euro. J. Pharma. Biopharm.* **57**, 263–267 (2004)
 26. Higuchi, T., Connors, K.: Phase solubility techniques. In: Reilly, C. (ed.) *Advances in Analytical Chemistry and Instrumentation*, pp. 117–212. Wiley–Interscience, New York (1965)
 27. Ronald, L.H., Jason, L.M., Krystle, A.Y., Julie, A.I.H., Kevin, A.W.: Inclusion complexes of cationic xanthene dyes in cucurbit[7]uril. *J. Incl. Phenom. Macrocycl. Chem.* **66**, 231–241 (2010)
 28. Christensen, M.B.V., Abouhachem, M., Svensson, B., Henriksen, A.: Crystal structure of an essential enzyme in seed starch degradation: barley limit dextrinase in complex with cyclodextrins. *J. Mol. Bio.* **405**, 739–750 (2010)
 29. Tonozuka, T., Sogawa, A., Yamada, M., Matsumoto, N., Yoshida, H., Kamitori, S., Ichikawa, K., Mizuno, M., Nishikawa, A., Sakano, Y.: Structural basis for cyclodextrin recognition by *Thermoactinomyces vulgaris* cyclo/maltodextrin-binding protein. *FEBS J.* **274**, 2109–2120 (2007)
 30. Gasteiger, J., Marsili, M.: Iterative partial equalization of orbital electro negativity a rapid access to atomic charges. *Tetrahedron* **36**, 3219–3228 (1980)
 31. Monica, R., Amrita, B., Ishwar, K., Ghanshyam, M., Francesco, T.: In vitro and in vivo evaluation of β -cyclodextrin-based nanosponges of telmisartan. *J. Incl. Phenom. Macrocycl. Chem* (2012)
 32. Powell, M.J.D.: Restart procedures for conjugate gradient method program. *Math. Prog.* **12**, 241–254 (1977)
 33. SYBYL7.1, Tripos Associates INC: S. Henley Rd., St. Louis, MO631444, USA. (1699)
 34. Frisch, M.J., Trucks, G.W., Schlegel, H.B., Scuseria, G.E., Robb, M.A., Cheeseman, J.R.: Gaussian-03 suite of programs. Gaussian Inc, Pittsburgh (2003)
 35. Emami, J.: In vitro-in vivo correlation: from theory to application. *J. Pharm. Pharmaceut. Sci.* **9**, 169–189 (2006)
 36. Patel, R.P., Patel, M.M.: Preparation and evaluation of inclusion complex of lipid lowering drug lovastatin with β -cyclodextrin. *Dhaka Univ. J. Pharm. Sci.* **6**, 25–36 (2007)
 37. Baglole, K. N., Boland, P. G., Wagner, B. D.: Fluorescence enhancement of curcumin upon inclusion into parent and modi
 38. Mark, E.D., Marcus, E.B.: Cyclodextrin-based pharmaceuticals: past, present and future. *Nat. Rev. Drug Discov.* **3**, 1023–1035 (2004)
 39. Krishna Mohan, P.R., Sreelakshmi, G., Muraleedharan, C.V., Joseph, R.: Water soluble complexes of curcumin with cyclodextrin: characterization by FT-Raman spectroscopy. *Vib. Spectrosc.* **62**, 77–84 (2012)
 40. Gupta, N.K., Dixit, V.K.: Bioavailability enhancement of curcumin by complexation with phosphatidyl choline. *J. Pharm. Sci.* **100**, 1987–1995 (2011)
 41. Kemp, D.C., Fan, P.W., Stevens, J.C.: Characterization of raloxifene glucuronidation in vitro: contribution of intestinal metabolism to pre-systemic clearance. *Drug Metab. Dispos.* **30**, 694–700 (2002)
 42. Wempe, M.F., Wachter, V.J., Ruble, K.M., Ramsey, M.G., Edgar, K.J., Buchanan, N.L., Buchanan, C.M.: Pharmacokinetics of raloxifene in male Wistar-Hannover rats: influence of complexation with hydroxybutenyl- β -cyclodextrin. *Int. J. Pharm.* **346**, 25–37 (2008)
 43. Lu, Y., Kim, S., Park, K.: In vitro-in vivo correlation: perspectives on model development. *Int. J. Pharm.* **418**, 142–148 (2011)
 44. Cardot, J.M., Beyssac, E., Alric, M.: In vitro–in vivo correlation: importance of dissolution in IVIVC. *Disso. Tech.* 15–16 (2007)
 45. Vinay, P., Raghu, G., Kusum, D., Roopa, S.P., Sarasija, S.: Preparation and characterization of Pioglitazone cyclodextrin inclusion complexes. *J. Young. Pharma.* **3**, 267–274 (2011)